Superconducting and Structural Properties of Strontium-Substituted $YBa_2Cu_4O_8$

P. Karen,[a] A. Kjekshus[a,*] and A. F. Andresen[b,†]

[a] Department of Chemistry, University of Oslo, Blindern, N-0315 Oslo 3 and [b] Institute for Energy Technology, N-2007 Kjeller, Norway

Karen, P., Kjekshus, A. and Andresen, A. F., 1992. Superconducting and Structural Properties of Strontium-Substituted $YBa_2Cu_4O_8$. – Acta Chem. Scand. 46: 1059–1064.

The $Y(Ba_{1-y}Sr_y)_2Cu_4O_{7.995\pm0.005}$ solid solution phase was prepared by syntheses at 800 °C in an ambient-pressure oxygen atmosphere, involving either a citrate precursor or reaction of CuO with $Y(Ba_{1-y}Sr_y)_2Cu_3O_7$. Both methods show a solid solubility limit of $y = 0.12(3)$, beyond which the latter two compounds emerge next to the major $YBa_2Cu_4O_8$-type phase. The solid solutions for $0.00 \leq y \leq 0.10$ were studied by means of powder X-ray and neutron diffraction at low and ambient temperature. No variation in T_c beyond 79.7(6) K is observed as a function of y, in sharp contrast to the behaviour of Sr-substituted $YBa_2Cu_3O_{6.95}$. For both solid-solution phases, searches for correlations between T_c and structural deformation and/or calculated valencies of the square-pyramidal Cu(2) atoms are performed. Comparisons with analogous effects of external pressure perturbation show that an increase in the Cu(2) valency caused by external pressure is consistently more effective in increasing T_c for both phases. A T_c detrimental effect, associated with the shift in the apical oxygen of the pyramid closer to Cu(2) [relative to the Cu(1) distance] is suggested as a possible additional effect to the T_c versus Cu(2)-valency correlation.

The synthesis[1] of the high-T_c superconductor $YBa_2Cu_4O_8$ (shorthand 124) permitted comparisons of its superconducting and structural properties with the earlier known, closely related $YBa_2Cu_3O_{7-\delta}$ (shorthand 123). The structural relationship involves merely inclusion of a CuO square chain in addition to that already existing in 123, so that the two chains in 124 share edges.[2,3] This largely prevents formation of oxygen vacancies,[4,5] and the rigid structure of 124, also resistant to oxygen content increase, represents a convenient matrix for examination of correlations between T_c and hole doping by aliovalent substitution.

The 124 phase possesses additional interesting features. Although T_c for 124 is only some 10 K lower than the 90 K for 123,[1] the superconducting behaviour shows striking differences. In particular, the pressure derivatives of T_c are disparate: while T_c as high as 108 K is reported[6] for 124 under high pressure, no larger increase than some 2 K is observed[7,8] by the application of external pressure on 123. Recently[9] it was concluded that at least a large component of the pressure variation of T_c for 123 is due to charge transfer from the Cu(1) square chains into the Cu(2) square-pyramidal sheets. This charge transfer was identified[10] as connected with an uniaxial (anisotropic) contraction of the structure fragment which contains the two Cu coordination polyhedra of different symmetries and bond lengths. Although such an anisotropy of the structural contraction could be roughly modelled using substitution of the larger Ba by the smaller Sr, the variation in T_c could not be simulated by the same approach,[11] even though a measure for the hole transfer from Cu(1) to Cu(2) is available from valence estimates from bond lengths.[10] This finding strongly suggests that another variable, related to structural parameters, may be in play, and an analogous investigation of the structural perturbation of 124 is accordingly of considerable interest.

Of the various reports on chemical substitutions in 124, two[12,13] concern the Sr for Ba substitution, but neither of these was aimed at detailed structural information. In the present study, structural parameters for $Y(Ba_{1-y}Sr_y)_2Cu_4O_{7.995(5)}$ prepared at 900 °C are refined from powder neutron diffraction (PND) and X-ray diffraction (PXD) data. Comparisons of the effects of external pressure[9,14] and Sr for Ba substitution[11] for both 123 and 124 are made in terms of structural deformation, interatomic distances and calculated copper valencies.

Experimental

Synthesis. Samples were prepared by firing of precursor materials obtained by liquid mixing in citrate gels. The starting components of a reagent grade or higher purity, *viz.* Y_2O_3 (5 N, Megon), $SrCO_3$ (5 N, Koch-Light), $BaCO_3$ (Merck) and $CuCO_3 \cdot Cu(OH)_2 \cdot 0.5H_2O$ (Riedel de Häen), were dissolved in boiling citric acid monohydrate (Fluka) to form a clear, blue, gel-like solution. The citrate gel was dehydrated at 180 °C, finely milled and incinerated in air at 450 °C. Pellets made from the powder obtained were sit-

* To whom correspondence should be addressed.
† Deceased.

uated on a protecting layer of powder of the same composition inside a corundum boat, which was subsequently placed into a tube furnace with a flowing oxygen atmosphere (10 l h^{-1}, purified on CuO at 600 °C and on KOH at ambient temperature). The firing at 800 °C for 150 h and at 340 °C for 6 h (except for the final treatment for 30 h) was repeated six times, with intermittent rehomogenizations.

Oxygen analysis. The oxygen content was determined iodometrically, based on analysis of the sample as such and compared with the sample prereduced by HCl. The use of finely milled samples, ultrasound agitation and an inert atmosphere ensured a reproducible and quantitative course of the solid–liquid reaction, while additions of NH_4SCN and soluble starch enhanced the accuracy of the titration. The reproducibility is better than ±0.005 in units of the formal oxidation state of copper.

Powder X-ray diffraction (PXD). All samples were characterized by PXD, using Guinier–Hägg cameras, Cu$K\alpha_1$ radiation and Si as internal standard. Positions and integrated intensities of the Bragg reflections were obtained by means of a Nicolet L18 film scanner and the SCANPI program system.[15] Unit cell dimensions were deduced by least-squares refinements[16] including only unambiguously indexable lines.

Powder neutron diffraction (PND). Neutron diffraction diagrams were obtained on the two-axis diffractometer OPUS III at the JEEP II reactor, Kjeller. Monochromatic neutrons of wavelength 187.7 pm were used, and diffraction data were collected in steps of $\Delta 2\theta = 0.05°$ between $2\theta = 5$ and 100°.

Least-squares refinements were carried out according to the Rietveld method[17] using the Hewat version[18] of the program. The scattering lengths $b_Y = 7.75$, $b_{Ba} = 5.25$, $b_{Sr} = 7.02$, $b_{Cu} = 7.72$ and $b_O = 5.81$ fm were used.[19] In the profile refinements, one common isotropic temperature factor was calculated for the metal atoms, since the small number of reflections and the large number of structural variables did not justify introduction of individual thermal parameters.

Low-temperature magnetic susceptibility. The a.c. induction method was adopted for determination of T_c and the Meissner effect of the superconducting samples. The powdered sample (50 mg) was placed into a cylindrical sample holder inside a field coil (300 Hz). The magnetic flux density at the sample site was approximately 1 mT. The voltage induced in the sample coils was amplified by a lock-in voltmeter (EG&G, model 5104 with a model 5004 ultra-low-noise preamplifier). Liquid nitrogen was used as a first-step coolant, whereas oxygen, condensed inside a sample chamber, was utilized for a second cooling step of the sample to the triple point of oxygen, upon evacuation of the chamber. After cooling in the field, the diamagnetic response of the superconductor was measured on increasing the temperature at a rate of 1 K min^{-1}. The temperature was measured at the sample position, with a type T, Cu–Cu/Ni thermocouple. The Meissner fraction was determined as an absolute value of dimensionless diamagnetic susceptibility (Dy_2O_3 was used as a paramagnetic standard). An apparent density of 4 g cm^{-3} was used to calculate the susceptibility per unit volume of the powder sample. For determination of T_c, the transition curves were tangentially extrapolated to zero at their inflexion points. At the read values of T_c, Meissner fractions less than 0.005 remained.

Results and discussion

Homogeneity region. Phase-pure (≥ 98 % according to PXD) $Y(Ba_{1-y}Sr_y)_2Cu_4O_8$ samples were prepared for y = 0.00, 0.05 and 0.10. When $y = 0.15$ and higher nominal substitution levels were attempted, the 123 phase and CuO appeared as impurities, and their amount did not change upon prolonged annealings. Neither can the higher substituted samples be prepared by a reaction of $Y(Ba_{1-y}Sr_y)_2Cu_3O_{6.95}$ with CuO, which otherwise proceeds well below $y = 0.15$. A conservative estimate of the limit for y for 800 °C and $P_{O_2} = 1$ atm is some $y = 0.12(3)$. This value is significantly lower than $y = 0.3$, reported for comparable conditions in Ref. 13 where, however, the increasing amounts of CuO with increasing content of Sr apparently were neglected. For higher temperatures and high pressures (1000 °C at P_{O_2} = 1000 atm), a limit of 0.40 is reported[12] for single or nearly single-phase samples. Unfortunately, the claimed oxygen contents between some 7.8 to 7.9 per formula unit are too low for single phase samples under the adopted preparative conditions. In this study, the formal copper valency is found constant (v = 2.2475 ± 0.0025), and the analyzed amount of oxygens per formula unit, 7.995 ± 0.005, is independent of the degree of substitution y.

Strutural properties. The substitution of Ba by the smaller Sr atom results in shortening of all three unit cell dimensions of $Y(Ba_{1-y}Sr_y)_2Cu_4O_8$. The contraction is slightly anisotropic, a least-squares approximation giving eqn. (1) (in

$$a = 384.2(1) - 8.6(31)y$$

$$b = 387.16(2) - 3.9(4)y$$

$$c = 7[389.15(2) - 6.6(5)y] \quad (1)$$

pm). The nature of this contraction is different from that in $Y(Ba_{1-y}Sr_y)_2Cu_3O_{6.95}$, where the highest shrinkage is observed for the long c-axis.[11]

The structural parameters were refined on the basis of the findings for non-substituted 124,[3] within the symmetry of space group *Ammm* (No. 65). The results are given in Table 1, for both 298 and 11 K, the labelling of the atoms in the chosen unit cell being evident from Fig. 1. The refined

Table 1. Structural parameters for $Y(Ba_{1-y}Sr_y)_2Cu_4O_8$ at 293 and 11 K (slanted) refined from PND data according to space group *Ammm*. Atomic coordinates (z), reliability factors R_N and unit cell parameters (in pm; 293 K data from PXD) are listed with standard deviations. Only a common overall isotropic temperature parameter was refined, $B \approx 4\times10^3$ pm^2.

Parameter	$y = 0.00$	$y = 0.05$	$y = 0.10$	Site
a	384.19(2)	383.63(3)	383.60(7)	
	383.4(1)	*383.2(1)*	*382.5(1)*	
b	387.15(2)	386.99(3)	386.75(3)	
	386.8(1)	*386.8(1)*	*386.3(1)*	
c	2724.1(1)	2721.5(2)	2719.6(2)	
	2715(1)	*2712(1)*	*2711(1)*	
$z_{Ba(Sr)}$	0.1370(5)	0.1371(6)	0.1371(5)	4h ($\frac{1}{2}$, $\frac{1}{2}$, z)
	0.1367(5)	*0.1363(6)*	*0.1365(5)*	
$z_{Cu(1)}$	0.2131(3)	0.2121(4)	0.2133(3)	4g (0, 0, z)
	0.2123(4)	*0.2123(6)*	*0.2133(4)*	
$z_{Cu(2)}$	0.0611(3)	0.0607(4)	0.0604(3)	4g (0, 0, z)
	0.0613(3)	*0.0616(4)*	*0.0618(4)*	
$z_{O(1)}$	0.1449(3)	0.1456(4)	0.1447(4)	4g (0, 0, z)
	0.1447(4)	*0.1439(5)*	*0.1438(4)*	
$z_{O(2)}$	0.0524(3)	0.0535(4)	0.0528(3)	4h ($\frac{1}{2}$, 0, z)
	0.0526(4)	*0.0535(5)*	*0.0531(3)*	
$z_{O(3)}$	0.0532(3)	0.0521(4)	0.0534(3)	4g (0, $\frac{1}{2}$, z)
	0.0537(4)	*0.0526(5)*	*0.0543(4)*	
$z_{O(4)}$	0.2195(3)	0.2189(4)	0.2192(3)	4g (0, $\frac{1}{2}$, z)
	0.2194(4)	*0.2183(4)*	*0.2185(3)*	
R_N	0.062	0.068	0.067	
	0.071	*0.080*	*0.078*	

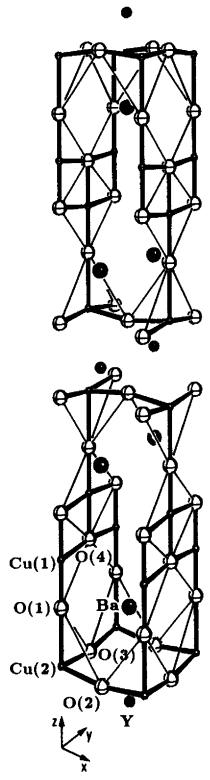

Fig. 1. Structural framework of 124. Location of the assymmetric unit of atoms is indicated, see also Table 1.

parameters for the non-substituted sample are in reasonable agreement with the precise data from the time-of-flight PND study by Lightfoot *et al.*,[20] obtained for a pressure-synthesized sample. Trends in selected interatomic distances, upon the change in the Sr for Ba substitution (y), follow from Table 2. Naturally, the contraction is centred at the Ba/Sr site, and all the Ba/Sr–O distances shorten. The Y–O bonds, however, remain constant or expand slightly. Parallel with this, the overall Cu–O framework contracts. Significant differences in behaviour are observed for the individual Cu–O distances. A uniform contraction is observed for the Cu–O distances which are (approximately) parallel to the short a- and b-axes. (Owing to the fixed position of Cu in the ab-plane, these distances follow the shrinkage of the cell edges.) The atomic interpretation of the contraction along the c-axis is more complex. Apparently as a compensation for the a- and b-axial compression of the copper–oxygen network, no significant contraction takes place for the c-parallel diagonals of the Cu(1) coordination squares. The adjacent apical distance of the Cu(2) square pyramid shows an interesting variation with y and temperature, a profound contraction being observed at 11 K as compared with the situation at room temperature. This feature follows as a consequence of the different behaviour of $x_{Cu(2)}$ as a function of the Sr for Ba substitution and temperature (Table 1). A corresponding feature is not observed for the Sr for Ba substitution in 123.[11]

Superconductivity. Virtually no variation in T_c with y occurs for $Y(Ba_{1-y}Sr_y)_2Cu_4O_8$, T_c = 80.0(3) 79.4(3) and 79.6(3) K being measured for y = 0.00, 0.05 and 0.10, respectively. In the same sequence, the Meissner fraction (for powdered samples) increases (0.15, 0.22 and 0.32 at 60 K), which is rather unusual, since a substitution is normally found to decrease the Meissner effect by the adopted measuring technique.[10,11,21] The susceptibility versus temperature characteristics for y = 0.00 and 0.05 show no stepwise behaviour, whereas a minor step with onset at 87.2 K is observed for the y = 0.10 sample. The magnitude of the step corresponds to a Meissner fraction of ~0.007, which could reflect an impurity of some 2 weight % $Y(Ba_{0.9}Sr_{0.1})_2Cu_3O_{6.95}$ in the sample (undetected by PXD). For comparison, T_c = 89.5 K and a Meissner fraction of 0.40 at 70 K were obtained for a reference sample of $YBa_2Cu_3O_{6.95}$, under the same conditions.

It is interesting to compare the structural and superconducting effects of the Sr for Ba substitution in 124 and 123. This comparison should also be supplemented by the information concerning the effect of external pressure, since both perturbations (*viz.* substitution and pressure; generally designated $\mathcal{P}$) affect neither the overall oxygen content nor the overall Cu valency.

Fig. 2 shows the effect of both kinds of perturbation on T_c for 123 and 124, related to the overall tetragonal or orthorhombic extensions relative to a single perovskite cell on the basis of unit cell parameters [eqn. (2) for 123 and eqn. (3) for 124]. No common correlation pattern is seen

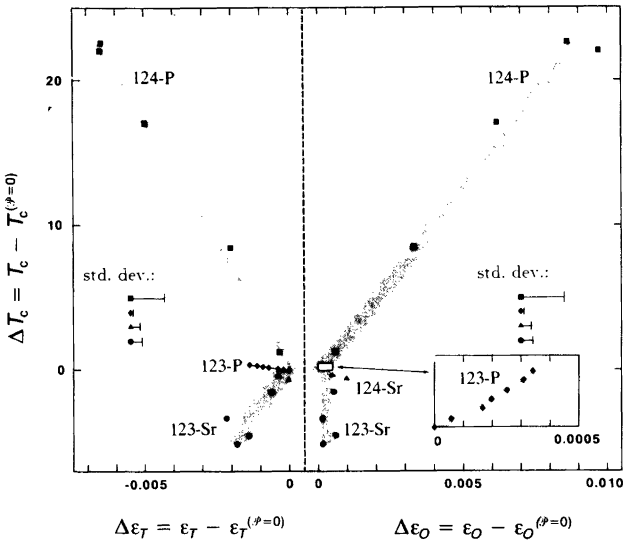

Fig. 2. ΔT_c and changes in tetragonal (left) and orthorhombic (right) extensions of the unit cell of 123 and 124 for various perturbations: Sr/Ba substitution in 123 (●)[11] and 124 (▲); application of external pressure on 123 (◆)[8,9] and 124 (■).[6,14,25] Regressed linearly by least squares from points weighted by their standard deviations. Widths of the shading correspond to standard deviations according to the regressions.

$$\varepsilon_T = 2c/3(a + b) \text{ and } \varepsilon_O = b/a \tag{2}$$

$$\varepsilon_T = 2c/7(a + b) \text{ and } \varepsilon_O = b/a \tag{3}$$

between T_c and these deformation parameters for the four situations under consideration.

In cuprates of the 123 type, T_c is usually[9,22] correlated with hole doping of the square-pyramidally coordinated Cu(2). The hole doping is simply expressed as the excess of formal Cu valency above 2, but its evaluation is not straightforward. Since two crystallographically non-equivalent and mixed-valent Cu atoms occur in these cuprates, perhaps the only passable way to establish individual Cu valencies is to make estimates from bond distances. We will follow here the procedure of Brown for estimation of formal valencies.[23,24] For the 123 phase there is a distinct correlation between T_c and the Cu(2) valency upon variation in oxygen content,[22] and a similar coherent pattern of correlations follows for the effects of external pressure[9] and some chemical substitutions.[10] An anomalous behaviour has, on the other hand, been observed[11] for the substitution of Ba by Sr, where T_c is decreased by the substitution, despite a calculated increase in the Cu(2) valency.

Ratios of formal valencies, eqn. (4), are calculated as

$$r = v_{Cu(2)}/v_{Cu(1)} \tag{4}$$

described elsewhere,[10] and are converted into Cu(2) valencies on the assumption that the overall Cu valency [i.e. $(2v_{Cu(2)} + v_{Cu(1)})/3$ for 123 and $(v_{Cu(2)} + v_{Cu(1)})/2$ for 124] remains constant, independent of $\mathcal{P}$ (as the formal va-

Table 2. Trends in selected interatomic distances (in pm) for $Y(Ba_{1-y}Sr_y)_2Cu_4O_8$ at 293 and 11 K (slanted). Slopes $\Delta D_{ij}/y$ and distances at zero substitution, $D_{ij;y=0}$ (with as regressed errors) refer to least squares fits weighted by standard deviations. Errors in interatomic distances are estimated by differentials assuming atomic coordinates independent. Note the distinction between the $D_{Cu(1)O(4)}$ distances parallel to *b* and *c*.

Atoms (*ij*)	*y* = 0.00	*y* = 0.05	*y* = 0.10	$\Delta D_{ij}/y$	$D_{ij;y=0}$
Ba–O(1)	273.56(19)	273.44(25)	273.15(22)	−4.0(8)	273.58(5)
	273.17(27)	*273.01(30)*	*272.53(25)*	*−6.5(17)*	*273.22(11)*
Ba–O(2)	301.0(17)	298.7(21)	299.9(17)	−10(18)	300.5(12)
	298.1(28)	*295.2(33)*	*296.1(25)*	*−18(19)*	*298.7(13)*
Ba–O(3)	298.3(17)	300.5(21)	297.7(17)	−7(25)	299.0(17)
	295.9(20)	*297.0(24)*	*293.7(19)*	*−22(23)*	*296.4(15)*
Ba–O(4)	295.6(17)	293.9(21)	294.3(17)	−13(11)	295.4(7)
	295.2(20)	*293.6(21)*	*293.2(17)*	*−19(7)*	*295.0(5)*
Cu(1)–O(1)	185.8(16)	181.1(22)	186.6(19)	+4(50)	184.8(31)
	183.5(22)	*185.5(30)*	*188.4(22)*	*+49(4)*	*183.4(3)*
Cu(1)–O(4)*c*	183.6(16)	187.8(23)	183.6(19)	+3(40)	184.4(24)
	185.4(22)	*188.2(30)*	*184.9(22)*	*−5(28)*	*186.0(19)*
Cu(1)–O(4)*b*	194.36(16)	194.38(22)	194.04(17)	−3.2(17)	194.40(11)
	194.36(27)	*194.08(28)*	*193.66(19)*	*−7.1(7)*	*194.38(5)*
Cu(2)–O(1)	228.3(19)	231.1(22)	229.3(19)	+10(24)	228.9(16)
	226.4(20)	*223.2(25)*	*222.3(23)*	*−42(12)*	*226.1(7)*
Cu(2)–O(2)	193.55(24)	192.81(24)	192.91(21)	−6(5)	193.4(3)
	193.15(28)	*192.86(33)*	*192.70(28)*	*−4.5(7)*	*193.13(5)*
Cu(2)–O(3)	194.77(19)	194.91(28)	194.31(18)	−4.7(31)	194.83(22)
	194.50(25)	*194.93(36)*	*194.22(28)*	*−2.6(54)*	*194.61(34)*
Cu(2)–Cu(2)	332.9(17)	330.4(22)	328.5(17)	−44(3)	332.8(2)
	332.9(20)	*334.1(26)*	*335.1(26)*	*+22(1)*	*332.9(1)*
Y–O(2)	240.5(5)	242.2(7)	240.9(5)	+4(14)	240.8(9)
	240.4(7)	*241.8(9)*	*240.9(6)*	*+4(10)*	*240.7(8)*
Y–O(3)	240.6(5)	238.5(7)	240.6(5)	−1(20)	240.2(13)
	240.8(7)	*238.9(9)*	*241.3(7)*	*+5(22)*	*240.3(15)*

Table 3. Trends in Cu(1) to Cu(2) charge transfer and in T_c upon various perturbations (pressure in GPa) for the 123 and 124 phases with constant formal Cu valency of 2.29(1).

Phase–Perturbation[a]	T/K	$\frac{\Delta r}{\Delta \mathcal{P}}$	r(0)	$\frac{\Delta v_{Cu(2)}}{\Delta \mathcal{P}}$	$v_{Cu(2)}(0)$	Range	$\frac{\Delta T_c}{\Delta \mathcal{P}}$
124–Sr	298	0.15(12)	0.931(8)	0.18(15)	2.098(10)	$0.0 < y < 0.1$	0
124–P(ressure)	298	0.004(2)	0.968(5)	0.005(2)	2.099(6)	$0.2 < P < 4.7^b$	5^c
123–Sr	298	0.10(7)	1.03(1)	0.07(4)	2.097(7)	$0.0 < y < 0.3^d$	$-18(3)^d$
123–P(ressure)	298	0.008(6)	1.028(2)	0.002(3)	2.118(2)	$0.0 < P < 0.6^e$	$0.65(15)^f$
124–Sr	11	0.5(2)	0.95(1)	0.6(2)	2.12(1)	$0.0 < y < 0.1$	
123–Sr	20	0.1(2)	1.07(4)	0.08(12)	2.12(2)	$0.0 < y < 0.3^d$	

[a]Perturbations: $\mathcal{P} \equiv y$ in $Y(Ba_{1-y}Sr_y)_2Cu_3O_{6.95}$ and $Y(Ba_{1-y}Sr_y)_2Cu_4O_8$; $\mathcal{P} \equiv$ external pressure P for $y = 0.00$; [b]Ref. 14; [c]Refs. 6 and 25; [d]Ref. 11; [e]Ref. 9; [f]Ref. 8.

lencies of Ba/Sr, Y and O clearly do). The results are regressed by the least-squares approach as linear functions of $\mathcal{P}$ and are listed in Table 3. Perhaps surprisingly, in both 123 and 124 the perturbations by Sr for Ba substitution and external pressure induce a hole transfer from Cu(1) to Cu(2). For a given kind of perturbation (Table 3), the most rapid increase in $v_{Cu(2)}$ occurs for 124, and this is paralleled in $\Delta T_c/\Delta \mathcal{P}$. This more sensitive response of 124 can be illustrated also by the fact that a much higher increase in T_c is obtained for 124 than for 123 by external pressure (in both cases, maxima in T_c are reached at the high-pressure end).[6,7]

Although the larger $\Delta v_{Cu(2)}/\Delta \mathcal{P}$-value for 124 may explain the different response of 124 and 123 to a given perturbation, the effects of the two kinds of perturbations on either phase are clearly disparate. When ΔT_c is plotted versus $v_{Cu(2)}$ (Fig. 3) the conclusion appears to be that hole doping by external pressure increases T_c more efficiently than hole doping by Sr for Ba substitution. However, a

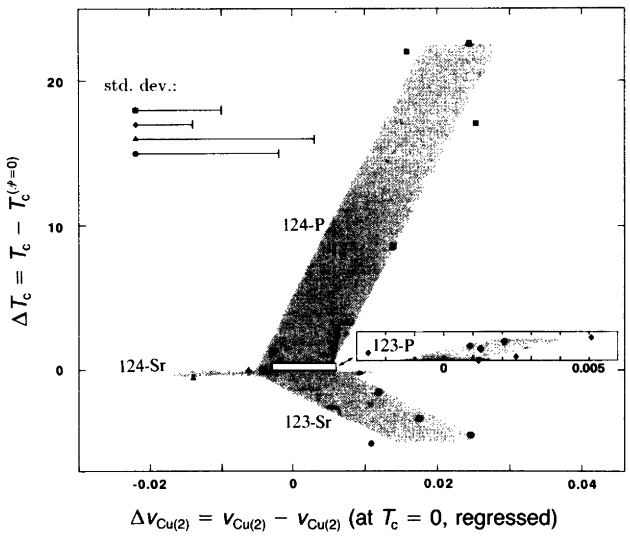

Fig. 3. ΔT_c and $\Delta v_{Cu(2)}$ for various perturbations of 123 and 124: Sr/Ba substitution in 123 (●)[11] and 124 (▲); application of external pressure on 123 (◆)[8,9] and 124 (■).[6,14,25] Regressed linearly by least squares from points weighted by their standard deviations. Widths of the shading correspond to standard deviations according to the regressions.

systematic drawback of the present approach (*de facto* valence calculations based on average bond distances) is that it does not respect the localized nature of the Ba for Sr replacements. Moreover, other structural effects correlated to T_c may be in play, which could introduce changes in the shape and location of the Fermi surface and thus affect T_c.

In order to gain further knowledge of the impact of structural effects of the charge transfer, valence ratios r [eqn. (4)] are calculated from the bond distance data in such manner that only distances specific to a particular anisotropic structural change are allowed to vary with the perturbation, while the remaining distances are constrained at their values for zero pertubation.[10] Bond distances parallel ($D_\parallel$) and perpendicular ($D_\perp$) to the c-axis of the unit cell, and for 123 also oxygen occupancies around the Cu(1) site ($n_{O(1)}$, $n_{O(5)}$) are chosen as variables, since they are likely to affect the charge transfer most distinctly.[10] The obtained estimates for partial differentials of the composite function r in terms of these pseudo-hypothetical variables are listed in Table 4. According to these disclosures, the charge transfer to Cu(2), which occurs for all perturbations, consists of a major contribution from $D_\perp$ and a smaller (comparable for 123-Sr) contribution from $D_\parallel$. The contribution from the slight changes in distribution of the oxygens in 123-Sr is negligible. The change in the $D_\perp$ distances due to the perturbations corresponds to an increase in ε_O. As discussed previously,[10] such an extension increases $v_{Cu(2)}$ for 123, since more bonds are being extended in the Cu(1) than Cu(2) coordination polyhedron (see also Fig. 1). The contribution from the $D_\parallel$ bonds to the charge transfer to Cu(2) is relatively simple to analyze, since, in principle, there are only two types of such bond distances: the Cu(2) apical bond (for 124: $D_{Cu(2)O(1)}$; Table 2) and the adjacent half-diagonal of the Cu(1) square [for 124: $(2D_{Cu(1)O(1)} + D_{Cu(1)O(1)c})/3$; Table 2]. As pointed out in Ref. 10, an approximate charge balance between the Cu(1) and Cu(2) sites would be maintained, when a variation in the diagonal distance is paralleled by an approximately seven times stronger response in the apical bond length. This condition is roughly fulfilled for the structural effects of external pressure on both 123 and 124 and for the effect of Sr substitution in 124, whereas Sr substitution in 123 causes

Table 4. Structural components of the Cu(1)–Cu(2) charge transfer and $\Delta T_c/\Delta\mathcal{P}$ upon various perturbations (pressure in GPa) for the 123 and 124 phases with constant formal Cu valency of 2.29(1). Structure data[a] at room temperature are used.

Phase–Perturbation[b]	$\frac{\Delta r}{\Delta\mathcal{P}}$	$\frac{\Delta r}{\Delta D_\parallel}\times\frac{\Delta D_\parallel}{\Delta\mathcal{P}}$	$\frac{\Delta r}{\Delta D_\perp}\times\frac{\Delta D_\perp}{\Delta\mathcal{P}}$	$\frac{\Delta r}{\Delta n}\times\frac{\Delta n}{\Delta\mathcal{P}}$	$\frac{\Delta T_c}{\Delta\mathcal{P}}$
124–Sr	0.15(12)	0.04(16)	0.11(4)		0
124–P(ressure)	0.0043(17)	−0.0021(14)	0.0065(5)		5
123–Sr	0.01(7)	0.05(6)	0.044(13)	−0.004	−18(3)
123–P(ressure)	0.008(6)	0.001(7)	0.0064(11)		0.65(15)

[a]References as Table 3. [b]Perturbations: $\mathcal{P} \equiv y$ in $Y(Ba_{1-y}Sr_y)_2Cu_3O_{6.95}$ and $Y(Ba_{1-y}Sr_y)_2Cu_4O_8$; $\mathcal{P} \equiv$ external pressure P for $y = 0.00$.

the apical distance to contract while the diagonal distance is expanded.

Since, as already mentioned, the correlations between charge transfer and T_c are not coherent for the four perturbed systems in question, it is somewhat surprising to learn from Table 4 that there is an apparent converse correlation between the $D_\parallel$ component of the charge transfer and ΔT_c for all perturbations: The larger $\Delta T_c/\Delta\mathcal{P}$ becomes, the smaller is the contribution of the *c*-parallel bonds to the charge transfer to Cu(2). Such a behaviour of the *c*-parallel bonds would require that the apical distance contracts least (or extends most), relatively to the contraction (or extension) of the adjacent diagonal of the square,[10] i.e. that T_c correlates positively with the apical oxygen departing from Cu(2).

This feature appears to indicate that the structural deformations give rise to impacts on T_c which are not directly related to the hole doping at Cu(2). Various terms involving absolute or relative (with respect to *a* and *b*) ratios of the apical and diagonal distances or of their perturbation differentials were tested for possible correlations with $\Delta T_c/\Delta\mathcal{P}$, in addition to the main dependence between T_c and $v_{Cu(2)}$. However, in relation to the large experimental errors and the uncertainty concerning whether or not the $T_c(v_{Cu(2)})$ relationships are the same for 123 and 124, the attempted calculations did not reveal more decisive information. Nevertheless, the qualitative evidence appears to suggest that there is an additional correlation between T_c and the position of the apical oxygen whose role[26] in stabilizing local singlet states[27] goes beyond the well established valency *versus* T_c relationship.

Acknowledgements. This work has received financial support from the Norwegian Council for Science and the Humanities (NAVF).

References

1. Karpinski, J., Kaldis, E., Jilek, E., Rusiecki, S. and Bucher, B. *Nature (London) 336* (1988) 660.
2. Kaldis, E., Fischer, P., Hewat, A. W., Hewat, E. A., Karpinski, J. and Rusiecki, S. *Physica C (Amsterdam) 159* (1989) 668.
3. Bordet, P., Hodeau, J. L., Argoud, R., Muller, J., Marezio, M., Martinez, J. C., Prejean, J. J., Karpinski, J., Kaldis, E., Rusiecki, S. and Bucher, B. *Physica C (Amsterdam) 162–164* (1989) 524.
4. Karpinski, J., Kaldis, E., Rusiecki, S., Jilek, E., Fischer, P., Bordet, P., Chaillout, C., Chenavas, J., Hodeau, J. L. and Marezio, M. *J. Less-Common Met. 150* (1989) 129.
5. Matthews, T. and Jacob, K. T. *Appl. Phys. Lett. 57* (1990) 511.
6. van Eenige, E. N., Griessen, R., Wijngaarden, R. J., Karpinski, J., Kaldis, E., Rusiecki, S. and Jilek, E. *Physica C (Amsterdam) 168* (1990) 482.
7. Klotz, S., Reith, W. and Shilling, J. S. *Physica C (Amsterdam) 172* (1991) 423.
8. Wijngaarden, R. J. and Griessen, R. In Narlikar, A. V., Ed., *Studies of High Temperature Superconductors, Advances in Research and Applications,* Nova Science Publishers, New York 1989, Vol. 2, pp. 29–77.
9. Jorgensen, J. D., Pei, S., Lightfoot, P., Hinks, D. G., Veal, B. W., Dabrowski, B., Paulikas, A. P. and Kleb, R. *Physica C (Amsterdam) 171* (1990) 93.
10. Karen, P., Fjellvåg, H. and Kjekshus, A. *J. Solid State Chem. 97* (1992) 257.
11. Karen, P., Fjellvåg, H., Kjekshus, A. and Andresen, A. F. *J. Solid State Chem. 92* (1991) 57.
12. Wada, T., Sakurai, T., Suzuki, N., Koriama, S., Yamauchi, H. and Tanaka, S. *Phys. Rev. B 41* (1990) 11209.
13. Liu, R. S., Ho, J. S., Chang, C. T. and Edwards, P. P. *J. Solid State Chem. 92* (1991) 247.
14. Nelmes, R. J., Loveday, J. S., Kaldis, E. and Karpinski, J. *Physica C (Amsterdam) 172* (1990) 311.
15. Werner, P. E. *The Computer Programme SCANPI,* Institute of Inorganic Chemistry, University of Stockholm, Sweden 1981.
16. Ersson, N. O. *Programme CELLKANT,* Chemical Institute, Uppsala University, Uppsala, Sweden 1981.
17. Rietveld, H. M. *J. Appl. Crystallogr. 1* (1968) 65.
18. Hewat, A. W. *UKAERE Harwell Rep.* RRL 73/897 (1973).
19. Koester, L. and Yelon, W. B. In Yelon, W. B., Ed., *Neutron Diffraction Newsletter,* The Neutron Diffraction Commission, Missouri, 1983.
20. Lightfoot, P., Pei, S., Jorgensen, J. D., Yamada, Y., Matsumoto, T., Izumi, F. and Kodama, Y. *Acta Crystallogr., Sect. C 47* (1991) 1143.
21. Andresen, P. H., Fjellvåg, H., Karen, P. and Kjekshus, A. *Acta Chem. Scand. 45* (1991) 698.
22. Cava, R. J., Santoro, A., Krajewski, J. J., Fleming, R. M., Waszczak, J. V., Peck, W. F., Jr. and Marsch, P. *Physica C (Amsterdam) 172* (1990) 138.
23. Brown, I. D. In: *Structure and Bonding in Crystals,* Academic Press, New York 1981, Vol. II, pp. 1–30.
24. Brown, I. D. *Phys. Chem. Miner. 15* (1987) 30.
25. Yamada, Y., Matsumoto, T., Kaieda, Y. and Mōri, N. *Jpn. J. Appl. Phys., Part 2, 29* (1990) L250.
26. de Jongh, L. J. *Eur. J. Solid State Inorg. Chem. 27* (1990) 221.
27. Ohta, Y., Tohyama, T. and Maekawa, S. *Phys. Rev. B 43* (1991) 2968.

Received March 4, 1992.